Rheology and Impact Characteristics of Compatibilized Polypropylene–Liquid Crystalline Polymer Composites

S. C. TJONG, R. K. Y. LI, Y. Z. MENG

Department of Physics and Materials Science, City University of Hong Kong, Tat Chee Avenue, Kowloon, Hong Kong

Received 29 December 1996; accepted 2 August 1997

ABSTRACT: Polypropylene–liquid crystalline polymer (PP/LCP) and maleic anhydride compatibilized PP/LCP blends were prepared using the extrusion technique followed by injection molding. The LCP employed was Vectra A950 which consists of 25 mol % of 2,6-hydroxynaphthoic acid and 75 mol % of *p*-hydroxybenzoic acid. The rheology, morphology, and impact behavior of compatibilized PP/LCP blends were investigated. The rheological measurements showed that the viscosity of LCP is significantly higher than that of the PP at 280°C. This implied that the viscosity ratio of the LCP to the polymer matrix is much larger than unity. Scanning electron microscopy (SEM) observations revealed that the LCP domains are dispersed mainly into elongated ellipsoids in the PP/LCP blends. However, fine fibrils with large aspect ratios were formed in the compatibilized PP/LCP blends containing LCP content $\geq$ 10 wt %. The development of fine fibrillar morphology in the compatibilized PP/LCP blends had a large influence on the mechanical properties. The Izod impact strength of the PP/LCP blends showed little dependence on the LCP concentrations. On the other hand, the impact strength of the compatibilized PP/LCP blends was dependent on the LCP concentrations. The correlation between the LCP fibrillar morphology and spherulitic structure with the impact properties of the compatibilized PP/LCP blends is discussed. J Appl Polym Sci **67:** 521–530, 1998

Key words: viscosity; polypropylene; liquid crystalline polymer; impact test; fibrillation

INTRODUCTION

There is a growing interest in the research of polyblends containing liquid crystalline polymers (LCPs) and thermoplastics. LCPs are composed of long-chain and rigid rodlike molecules that exhibit an ordered structure in the melt. Oriented LCPs relax very slowly due to the rotation of whole molecules or the cooperative movement of many molecular segments. In this case, the orientation developed in the molten state can be preserved after solidification. LCPs are being actively studied in the 5–40% composition range for thermoplastics, in view of their potential as processing aids and reinforcing agents.[1–9] This is due to melt viscosity reduction resulting from the addition of small amounts of LCP. In addition, the LCPs can deform into elongated fibrils under adequate processing conditions; such fibrils tend to reinforce the thermoplastic matrix, thereby creating the *in situ* polymer composites.

For the effective transfer of stress from the matrix to reinforcement, the dispersed phase of LCP/thermoplastic blends should exhibit a fibrillar structure.[10–12] However, it is found that the LCP domains do not always deform into fibrils for some LCP/thermoplastic blends. In this case, the LCPs are usually in the form of spherical droplets and

Correspondence to: S. C. Tjong.

Journal of Applied Polymer Science, Vol. 67, 521–530 (1998)
 CCC 0021-8995/98/030521-10

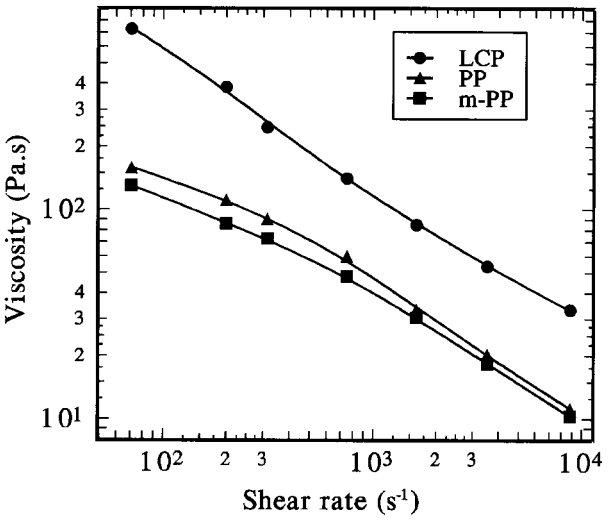

Figure 1 Viscosity as a function of shear rate for LCP, PP, and *m*-PP at 280°C.

ellipsoids.[13] The morphology of the LCP dispersed phase in LCP/thermoplastics blends has been reported to vary depending on the flow mode, viscosity ratio, interfacial tension, and blend composition. Extensional flow is believed to be more effective than shear flow to elongate LCP domains into a fibrillar structure.[14] In injection-molding processes, the effect of flow on the deformation of the LCP dispersed phase is more complex. A skin–core morphology usually developed in the molded parts. Highly oriented fibrils are found in the skin layer whereas a less oriented LCP phase is observed in the core region. The high-degree orientation in the skin region results from the extensional flow at the advancing flow front while less orientation in the core region arises from the shear flow in the center of the mold.[15] In addition, the viscosity ratio between the LCP and polymer matrix plays a crucial role in the fibrillation of LCP. The viscosity ratio of the LCP dispersed phase to the matrix polymer must be closer to unity or less for the production of an *in situ* composite. Beery et al.[2] investigated the fibril development during the capillary flow of LCP/thermoplastic blends. The thermoplastics used were poly(butylene terephthalate) (PBT), polycarbonate (PC), and polyamide 6 (PA6). They reported that a fibrillar structure is developed in the PC/LCP system where the viscosity of the polymer matrix is higher than the LCP. However, spherical LCP particles are observed in the PBT/LCP blends where the viscosity of PBT is lower than that of the LCP.

LCP/thermoplastic blends are reported by several workers to be immiscible or incompatible. The poor adhesion between the LCP dispersed phase and the matrix polymer leads to polyblends that exhibit poor tensile strength and modulus. A number of studies have been carried out to improve the compatibility of LCP and the matrix polymer. These include modification of the LCP molecular structure by incorporating long flexible spacer groups in the main chain[16] and introduction of a graft copolymer with segments capable of specific interactions with the blend components.[17–20] In the latter case, Miller et al.[17] employed an acrylic acid-functionalized polypropylene (PP) as a compatibilizer for PP/LCP polyblend fibers. They re-

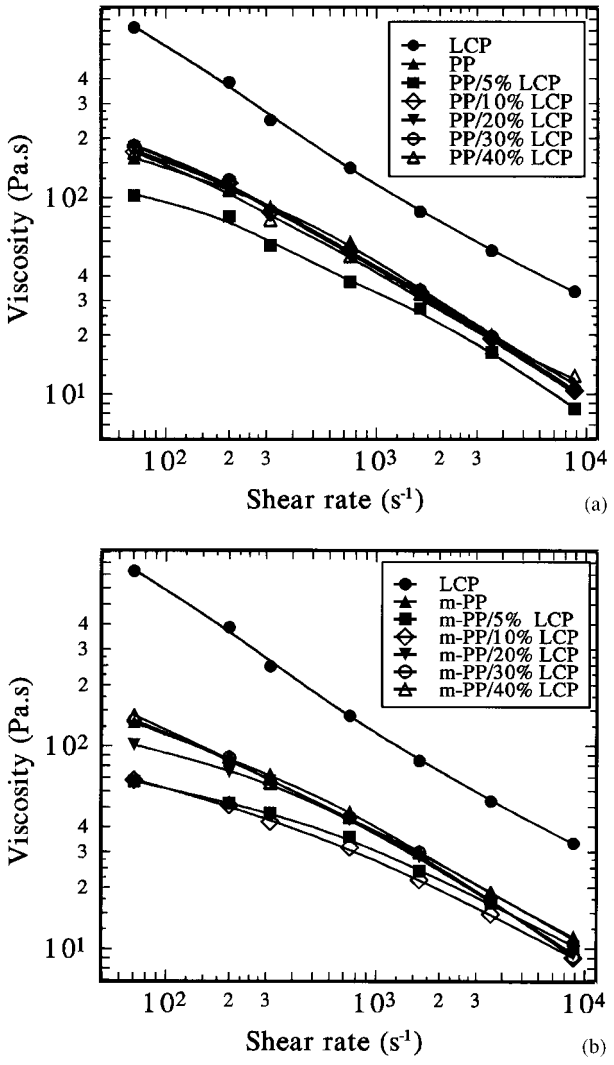

Figure 2 Viscosity as a function of shear rate for (a) PP/LCP and (b) *m*-PP/LCP blends at 280°C.

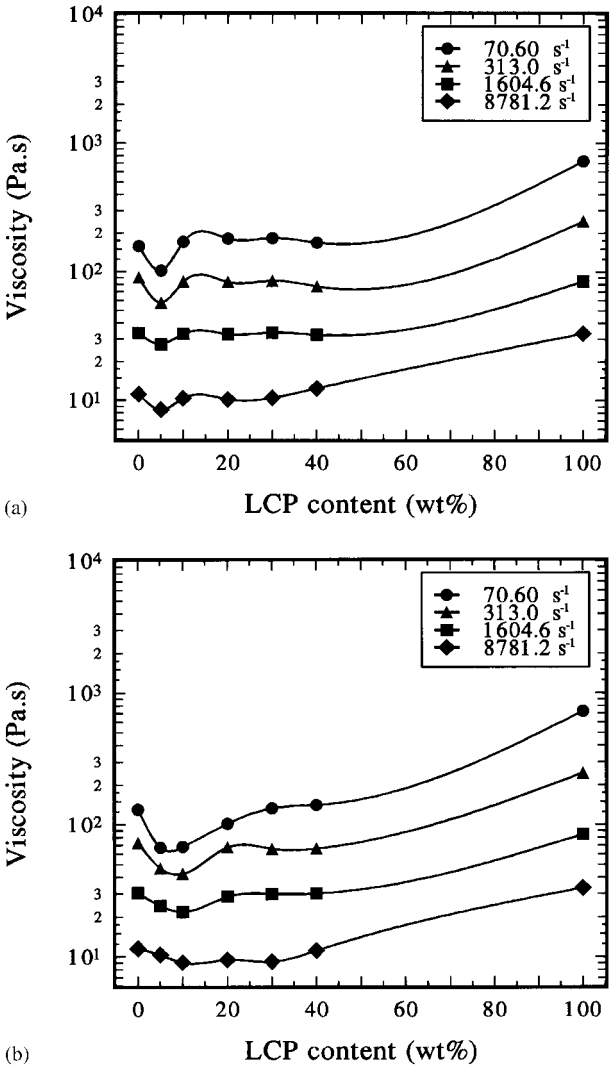

Figure 3 Viscosity as a function of LCP concentration for (a) PP/LCP and (b) *m*-PP/LCP blends at 280°C.

ported that the functional compatibilizer tends to improve the interfacial adhesion, thereby promoting higher fiber crystallinity and mechanical properties. They attributed the improvement in adhesion to the existence of an interaction between the polar acrylic acid groups and the LCP. In another study, Chiou et al.[18] applied a reactive compatibilizer based on the ethylene–glycidyl methacrylate copolymer (EGMA) for the PP/LCP blends. The epoxy functional groups of the EGMA copolymer can react with the carboxylic acid and/or the hydroxyl end groups of the liquid crystalline copolyester. Consequently, the compatibilized PP/LCP blends showed finer dispersed LCP domains but lower PP crystallinity. More recently, Baird and coworkers studied the tensile properties of maleic anhydride-grafted polypropylene (MAP) compatibilized PP/LCP blends. They observed significant improvements in the tensile modulus but a reduced tensile elongation in the compatibilized PP/LCP blends.[19,20] They suggested that interaction such as hydrogen bonding between MAP and LCP is responsible for the compatibilizing effect of MAP on PP/LCP blends. However, no detailed analyses of the rheological properties, crystallization kinetics, and impact behavior of the MAP compatibilized PP/LCP blends were conducted by Baird et al. As part of our study on the development of fibrillar structure in PP/LCP blends, this article aimed to study the effect of MAP compatibilization on the flow properties and impact behavior of PP/LCP blends. The impact test results obtained from this work will correlate with the crystallization kinetics behavior of the MAP compatibilized PP/LCP blends reported previously.[21]

EXPERIMENTAL

Materials and Method of Investigation

The thermotropic LCP used in this work was Vectra A950 produced by the Hoechst-Celanese Co. Vectra A950 is a wholly aromatic copolyester consisting of 25 mol % of 2,6-hydroxynaphthoic acid (HNA) and 75 mol % of *p*-hydroxybenzoic acid (HBA). The PP matrix is a commercial product of the Himont Co. (Profax 6331) with a melt flow index of 12. The compatibilizer is a

Table I Values of Viscosity Ratio Between the LCP and PP at 280°C

	Shear Rate (s^{-1})						
	70.6	199.8	313	748.8	1604.6	3513	8781.2
Viscosity ratio	4.59	3.46	2.74	2.36	2.54	2.64	2.96

Table II Values of Viscosity Ratio Between the LCP and *m*-PP at 280°C

	Shear Rate (s^{-1})						
	70.6	199.8	313	748.8	1604.6	3513	8781.2
Viscosity ratio	5.57	4.49	3.39	2.95	2.78	2.92	3.22

maleic anhydride (MA) supplied by Fluka Chemie, whereas dicumyl peroxide produced by the Aldrich Chemical Co. is used for the maleation of PP.

Maleation was performed by mixing 6 wt % MA and 0.3 wt % dicumyl peroxide with PP pellets in a twin-screw Brabender extruder at 200°C. The extrudates were then granulized and are designated as *m*-PP in this work. The *m*-PP and LCP pellets were dried in an oven at 70 and 150°C for 24 h, respectively, prior to use. The *m*-PP/LCP blends containing 5, 10, 20, 30, and 40 wt % LCP were prepared again in the Brabender. The barrel temperatures from root to die were maintained at 290, 295, 295, and 290°C, respectively. A similar procedure was adopted to prepare noncompatibilized PP/LCP blends. Finally, both *m*-PP/LCP and PP/LCP blend pellets were injection-molded into rectangular plaques with 6 mm thickness and standard dog-bone tensile bars (ASTM D638). The barrel zone temperatures were set at 280°C, whereas the mold temperature was maintained at 50°C.

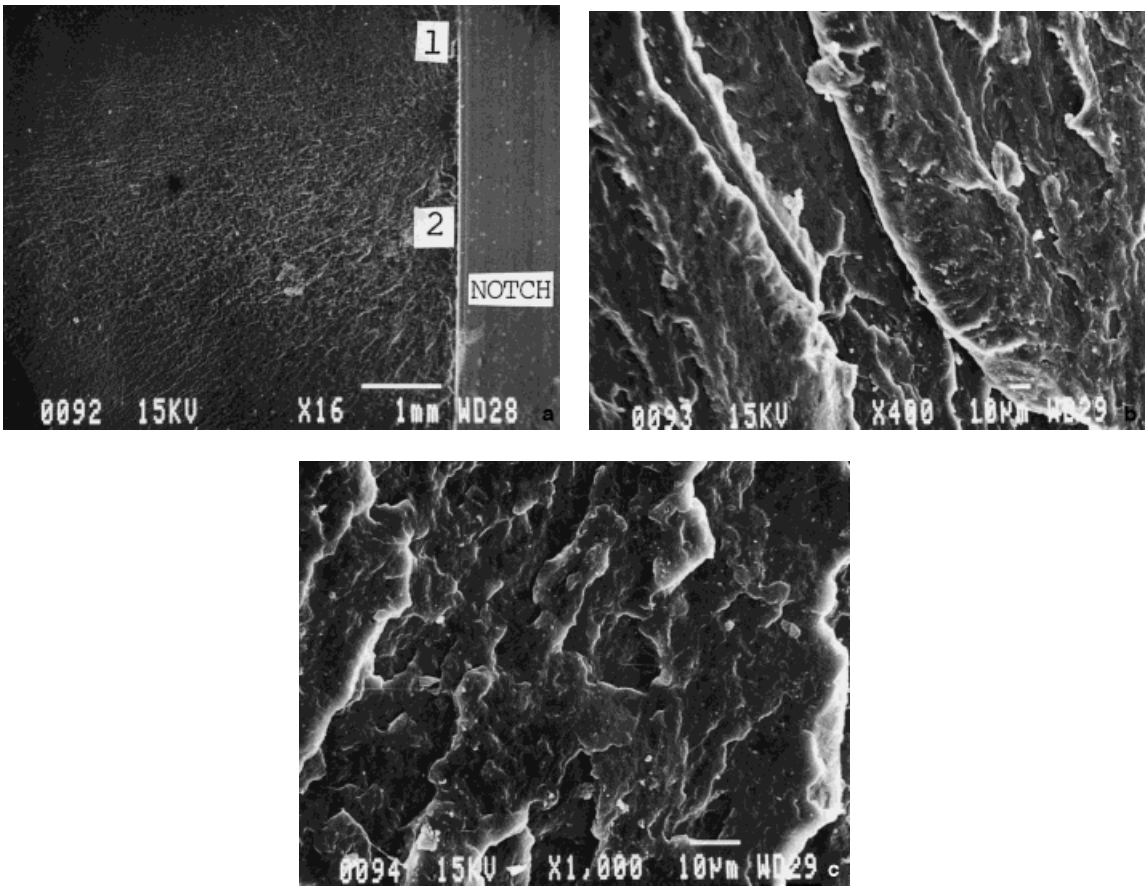

Figure 4 (a) Low-magnification SEM micrograph of the fracture surface of pure PP after impact test; (b) higher magnification fractograph of region 1; (c) higher-magnification fractograph of region 2 as marked in (a).

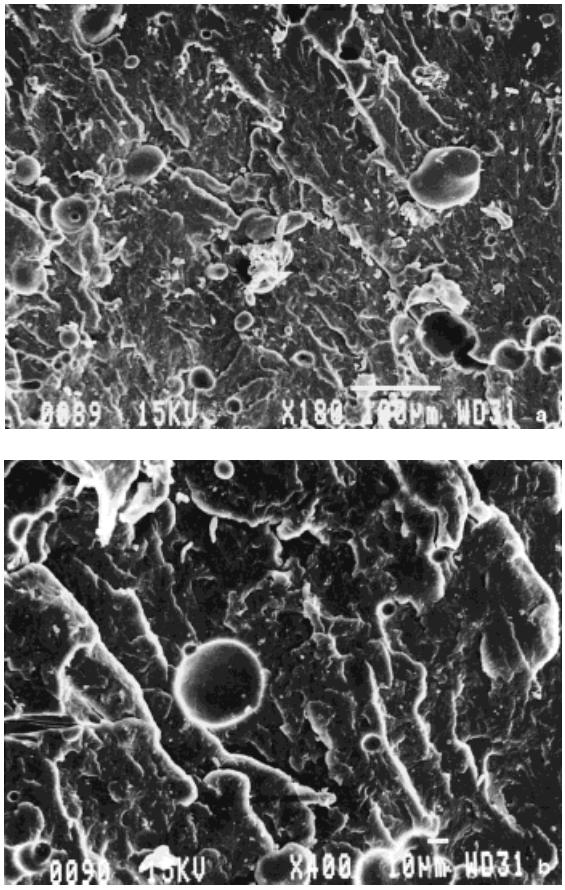

Figure 5 SEM micrographs showing the fracture surface of (a) skin section and (b) core region of the PP/10% LCP blend after impact test.

Izod impact specimens with dimensions of 63 $\times$ 13 $\times$ 6 mm were prepared from the plaques and they were tested using an Ceast impact pendulum tester. Reported values are the average of five measurements. The fracture surfaces of impact specimens were examined in a scanning electron microscope (SEM, JEOL Model 820). They were coated with a thin layer of gold prior to SEM observations.

The flow behavior of the blends investigated was studied using a Rheograph capillary rheometer (Model 2003). The capillary had a 1 mm diameter and was 30 mm long (L/D = 30). Measurements were taken at 280°C over a wide range of shear rates.

RESULTS AND DISCUSSION

Rheological Behavior

Figure 1 shows the rheological behavior of the LCP, PP, and *m*-PP at 280°C. It can be seen that the LCP, PP, and *m*-PP specimens exhibit non-Newtonian and shear thinning behavior over a large range of shear rates. The viscosity curves of PP/LCP and *m*-PP/LCP blends are shown in Figure 2(a) and (b), respectively. Apparently, these figures reveal that the viscosity of the LCP extruded at 280°C is significantly higher than that of PP and *m*-PP. Furthermore, the flow curves of LCP and PP do not intersect. From Figure 2(a), it is noticed that the viscosities of the blends are lower than those of the pure components. The PP/LCP blend containing 5% LCP has the lowest viscosity over the entire range of shear rates studied. The variation of melt viscosity with the LCP content for the PP/LCP and *m*-PP/LCP blends are shown in Figure 3(a) and (b). It can be seen from Figure 3(a) that the viscosities of the PP/LCP blends extruded at various shear rates reach a minimum at 5% LCP content; thereafter,

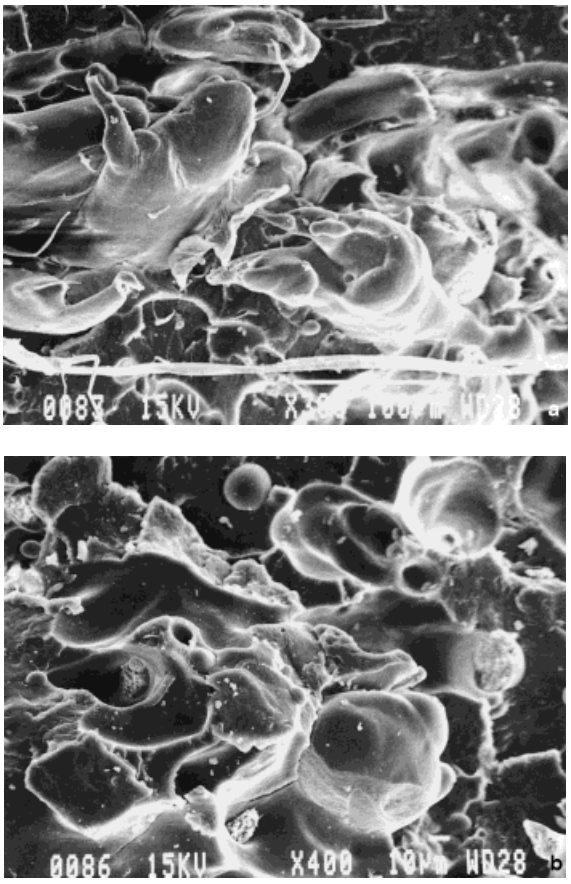

Figure 6 SEM micrograph showing the fracture surface of (a) skin section and (b) core region of the PP/40% LCP blend after impact test.

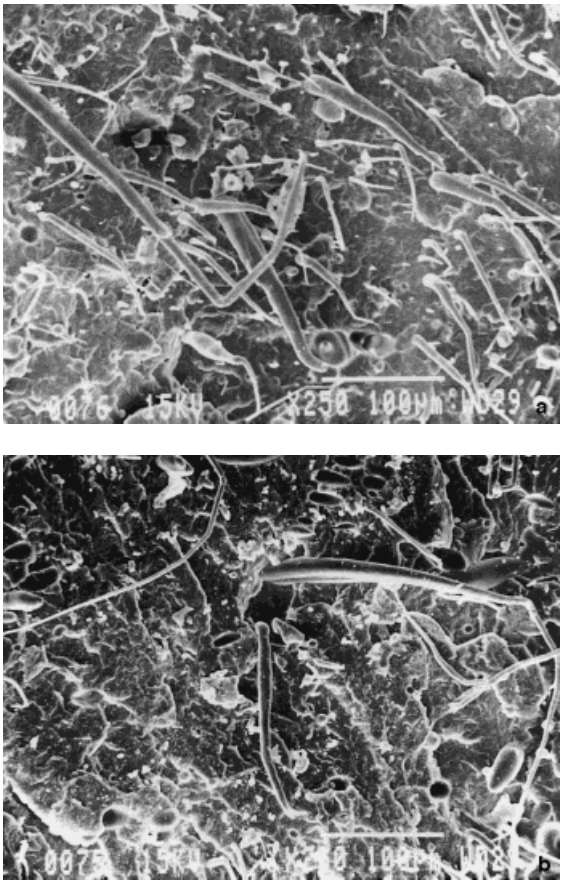

Figure 7 SEM micrograph showing the fracture surface of (a) skin section and (b) core region of the *m*-PP/10% LCP blend after impact test.

they tend to increase slightly and approach a steady-state condition when the LCP content reaches 40 wt %.

It is generally known that LCP domains can deform into fibrils when their viscosity is less than that of the matrix polymer. Thus, LCP fibrillation occurs when the viscosity ratio of the LCP to the polymer matrix is smaller or closer to unity.[22] For example, long fibrils have been observed in the LCP/poly(phenylene ether) blends as the viscosity of LCP is significantly lower than that of the host resin.[23,24] In this work, the viscosity of the LCP is much higher than that of the PP or *m*-PP. This means that LCP fibrillation is unlikely to occur in PP/LCP or *m*-PP/LCP blends. Tables I and II summarize the viscosity ratios of LCP to the matrix polymer for PP/LCP and *m*-PP/LCP blends at 280°C. These tables show that the viscosity ratios of both PP/LCP and *m*-PP/LCP blends tend to decrease with increasing shear rates. Nevertheless, these ratios are still much larger than unity even at a very high shear rate of 8781.2 s^{-1}. Moreover, the viscosities ratios of LCP to the polymer matrix for the *m*-PP/LCP blends are considerably higher than those of the PP/LCP blends. Thus, the chance of forming LCP fibrils in *m*-PP/LCP blends is smaller than in the PP/LCP blends. However, SEM fractography demonstrates that long LCP fibrils are formed in the matrix of *m*-PP/LCP blends containing LCP content $\geq$ 10% as mentioned in the next section. Thus, other factors such as the relaxation effect of polymers must be taken into consideration for LCP fibrillation.[25] Castelum and Wagner[26] reported that the viscosity ratio of LCP/PP is much less than unity as the LCP exhibits a much lower viscosity than does PP processed at 275°C. Thus, LCP fibrils were

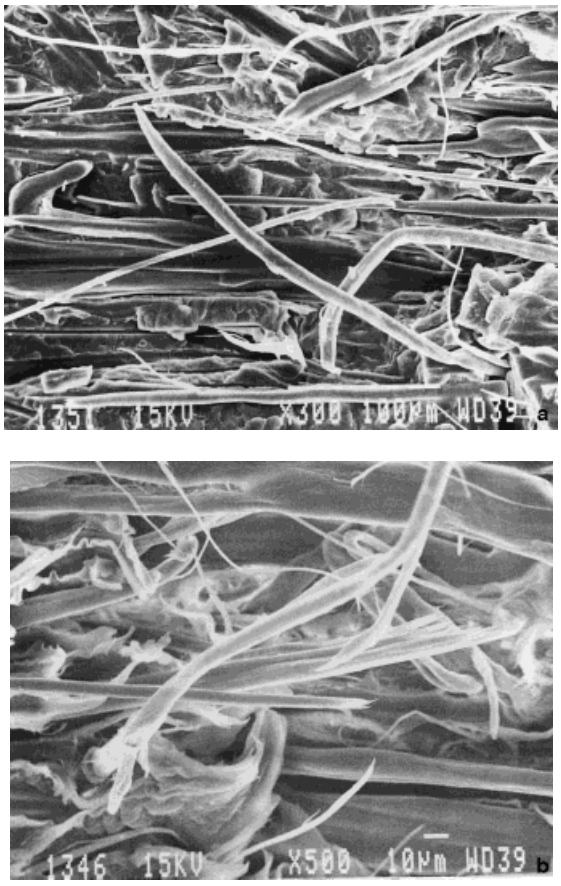

Figure 8 SEM micrographs showing the fracture surface of skin section of (a) *m*-PP/20 LCP and (b) *m*-PP/40% LCP blends after impact test.

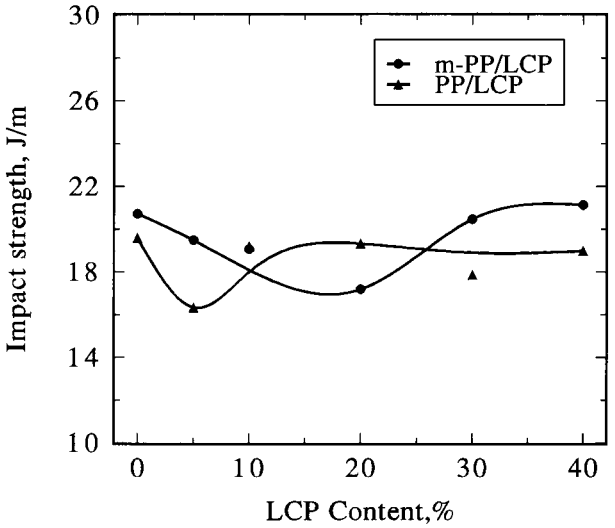

Figure 9 Variation of Izod impact strength with LCP content for the PP/LCP and *m*-PP/LCP blends.

formed in the uncompatibilized PP/LCP blends. It should be noted that the LCP used by them was LC-3000 (Rodrun, Unika) which consists of 60% *p*-hydroxybenzoic acid and 40% poly(ethylene terephthalate).

Fractography

Figure 4(a) shows a low magnification fractograph of pure PP after the impact test. Higher-magnification SEM micrographs of the skin and core regions [marked 1 and 2 in Fig. 4(a)] next to the notch of pure PP are shown in Figure 4(b) and (c), respectively. The micrographs shows that the fracture surfaces of PP next to the notch are relatively smooth, indicating that little plastic deformation has taken place in these regions during the impact tests. This is due to that PP generally exhibits low-impact strength in the presence of a notch. Figure 5(a) and (b) show SEM fractographs of the PP/10LCP blends taken at the skin and core regions. The LCP domains appear as both spherical droplets and ellipsoids in the skin layer [Fig. 5(a)], whereas they remain as spherical particles in the core region [Fig. 5(b)]. Further increasing the LCP content to 40% still results in the formation of predominant ellipsoids in the skin region [Fig. 6(a)]. Only a few fibers can be seen in this micrograph. The morphology of the core region of the PP/40% LCP blend is characterized by the formation of spherical LCP domains [Fig. 6(b)]. On the other hand, fine fibrils are observed in the skin region of the *m*-PP/10LCP blend [Fig. 7(a)]. In the core region, both fine fibrils and elongated ellipsoids are observed [Fig. 7(b)]. Furthermore, long and fine fibrils with large aspect ratios are seen within the matrix of *m*-PP/20LCP and *m*-PP/40LCP blends [Fig. 8(a) and (b)]. Thus, the MAP addition leads to a much finer dispersion of LCP domains in the matrix polymer. It is considered that a hydrogen-bonding interaction between the *m*-PP and LCP improves the interfacial adhesion between them, thereby promoting better dispersion of the LCP phase.[19,20]

Impact Properties

Figure 9 shows the variation of the notch impact strength of the PP/LCP and the *m*-PP/LCP blends. The impact energy of the PP/LCP blends shows little dependency on the LCP content. However, the impact strength of the *m*-PP/LCP blends appears to decrease initially with increasing LCP content. As the LCP content reaches 30 wt % or greater, the impact energy tends to increase with increasing LCP concentration. In this case, the impact behavior of *m*-PP/LCP blends is similar to that of the glass fiber-reinforced polymer com-

Table III Kinetic Parameters for Nonisothermal Crystallization of PP/LCP Blends Determined at 105°C

PP/LCP	T_m (°C)	$T_{1/2}$ (°C)	n	X_c	$K(T_{1/2})$
100/0	168	105	4	0.44	4.33×10^{-6}
95/5	167	106	3.7	0.48	1.07×10^{-5}
90/10	167	108	3.8	0.48	7.90×10^{-5}
80/20	166	108	3.8	0.53	7.90×10^{-5}
70/30	168	107	3.8	0.55	7.90×10^{-5}
60/40	170	108	3.8	0.61	7.90×10^{-5}

Table IV Kinetic Parameters for Nonisothermal Crystallization of *m*-PP/LCP Blends Determined at 105°C

m-PP/LCP	T_m (°C)	$T_{1/2}$ (°C)	n	X_c	$K(T_{1/2})$
100/0	165	107	4	0.43	4.33×10^{-6}
95/5	167	109	3.7	0.45	1.07×10^{-5}
90/10	168	108	3.6	0.46	1.43×10^{-5}
80/20	168	108	3.5	0.47	1.93×10^{-5}
70/30	169	110	3.4	0.45	2.61×10^{-5}
60/40	167	109	3.4	0.48	2.61×10^{-5}

posites. This behavior is due to the fact that LCP domains can deform into a fine fibrillar structure in the *m*-PP/LCP blends, thereby promoting the formation of *in situ* polymer composites. Therefore, the LCP fibrils reinforce the polymer matrix of *m*-PP/LCP effectively. It is generally known that the impact toughness of the polymer composites tends to decrease with increasing fiber content. However, it has been reported that the notched impact toughness and the plane strain fracture toughness (K_{IC}) of the thermoplastics can be increased markedly by adding a sufficient amount of glass fibers, i.e., above 30 wt %.[27,28] The improvement in fracture toughness is believed to originate from an enhanced matrix plasticity at the fiber ends in the crack-tip region when the glass fibers are closely spaced. It is noticed from Figure 9 that the improvement in the impact toughness of *m*-PP/LCP *in situ* composites containing an LCP content $\geq$ 30% is considerably smaller than that of the glass fiber-reinforced polymer composites.

It should be noted that the improvement of the mechanical properties of the *m*-PP/LCP blends can also be related to the development or growth of spherulites in the polymer matrix of the *m*-PP/LCP blends. It is likely that the semicrystalline PP would interact with the oriented LCP component during solidification. The LCP domains may provide nucleating sites for crystallization, leading to epitaxial growth. It is generally known that the crystallization behavior of polymers would influence their impact and tensile properties significantly.[29,30] The isothermal and nonisothermal kinetics of the PP/LCP and *m*-PP/LCP blends were investigated recently by Tjong et al.[21] They reported that the nonisothermal kinetics parameters determined from the Ozawa equation are in good agreement with those determined from the isothermal kinetics parameters calculated from the Avrami equation. The values of the Ozawa exponent of the PP/LCP blends are identical to those of the Avrami exponent. The nonisothermal crystallization kinetics is of particular importance as most of the polymers are processed under nonisothermal crystallization conditions. The Ozawa equation is generally used to describe the nonisothermal crystallization behavior of polymers,

$$X(T) = 1 - \exp[-K(T)/C^n] \quad (1)$$

where $X(T)$ is the crystallinity at temperature T; $K(T)$, the rate constant; C, the cooling rate; and n, the Ozawa exponent.[31] The parameters n and $K(T)$ are determined from the double logarithmic form of the Ozawa equation:

$$\ln\{-\ln(1 - X(T))\} = \ln K(T) + n \ln(1/C \quad (2)$$

The Ozawa exponent is normally used to characterize the growth order of the spherulites during the nonisothermal crystallization process. A more precise method to determine $K(T)$ involves the use of $T_{1/2}$, which is the temperature where the 50% of the crystalline phase has been attained. Taking the logarithm of eq. (1) at $T = T_{1/2}$, we obtain

$$K(T_{1/2}) = \ln 2/C^n \quad (3)$$

Tables III and IV list the kinetics parameters for nonisothermal crystallization of PP/LCP and *m*-PP/LCP extrudates, respectively.[21] It can be seen from Table III that the Ozawa exponent (n) of pure PP is 4, while the Ozawa index for the PP/LCP blends is 3.8. On the other hand,

the Ozawa exponent of *m*-PP is also 4, while values of $n = 3.4–3.7$ were found for the *m*-PP/LCP composites. The Avrami exponent of 4 can be interpreted as homogeneous nucleation of the spherulites from the melt during the crystallization process followed by three-dimensional growth. However, heterogeneous nucleation and three-dimensional spherulitic growth led to an Avrami exponent of 3. From Tables III and IV, it is evident that the spherulites nucleate homogeneously from the melt for the PP/LCP blends. Hence, the LCP does not provide a nucleation site for the spherulites. The LCP provides a nucleation site only for the *m*-PP/LCP blends. Engberg et al. also reported that the crystallization of semicrystalline poly(butylene terephthalate) was unaffected by the presence of LCP.[32] In addition, it is worth noting that the transcrystalline spherulitic growth is observed only in the *m*-PP/LCP blends.[21] The presence of transcrystalline regions may improve the mechanical properties of some fiber-reinforced polymer composites.[33,34] Moreover, Tables III and IV also reveal that the values of the rate constant $[K(T_{1/2})]$ of the *m*-PP/LCP blends containing LCP $\geq$ 10% are generally smaller than those of the corresponding PP/LCP blends. In this regard, the addition of LCP to the maleated PP tends to increase the overall crystallization rate owing to that the LCP fibrils provide heterogeneous nucleation sites for the spherulites.

CONCLUSIONS

1. The rheological measurements show that the viscosity ratios of PP/LCP and *m*-PP/LCP blends at 280°C are much larger than unity for all the shear rates studied.
2. SEM observations reveal that the LCP domains mainly exhibit ellipsoid morphology for the PP/LCP blends containing higher LCP concentrations. However, extended fine LCP fibrils are formed in the polymer matrix of the *m*-PP/LCP blends containing an LCP content $\geq$ 10 wt %.
3. The Izod impact tests show that the impact energy of PP/LCP blends shows little dependency on the LCP concentrations. However, the impact strength of *m*-PP/LCP blends initially decreases with increasing LCP content followed by an increase at higher LCP concentrations. These are the typical impact characteristics of fiber-reinforced composites.
4. The heterogeneous nucleation and transcrystalline growth of spherulites are also responsible for the improvement in impact properties of *m*-PP/LCP blends with higher LCP concentrations.

The authors would like to thank Mr. S. X. Chen for assistance in the impact measurements.

REFERENCES

1. T. M. Malik, P. J. Carreau, and N. Chapleau, *Polym. Eng. Sci.,* **29,** 600 (1989).
2. D. Beery, S. Kenig, and A. Siegmann, *Polym. Eng. Sci.,* **31,** 451 (1991).
3. A. Mehta and A. I. Isayev, *Polym. Eng. Sci.,* **31,** 971 (1991).
4. W. C. Lee and A. T. Dibenedetto, *Polym. Eng. Sci.,* **32,** 400 (1992).
5. H. Verhoogt, H. C. Langelaan, J. Van Dam, and A. P. De Boer, *Polym. Eng. Sci.,* **33,** 754 (1993).
6. S. C. Tjong, S. L. Liu, and R. K. Y. Li, *J. Mater. Sci.,* **30,** 353 (1995).
7. S. C. Tjong, S. L. Liu, and R. K. Y. Li, *J. Mater. Sci.,* **31,** 479 (1996).
8. S. C. Tjong, J. S. Shen, and S. L. Liu, *Polym. Eng. Sci.,* **36,** 797 (1996).
9. L. Mascia and L. H. Martin, *High Perform. Polym.,* **8,** 119 (1996).
10. G. Kiss, *Polym. Eng. Sci.,* **27,** 410 (1987).
11. D. E. Turek and G. P. Simon, *Polymer,* **34,** 2750 (1993).
12. J. P. de Souza and D. G. Baird, *Polymer,* **37,** 1985 (1996).
13. P. R. Subramanian and A. I. Isayev, *Polymer,* **32,** 1961 (1991).
14. G. C. Viola, D. G. Baird, and G. L. Wilkes, *Polym. Eng. Sci.,* **25,** 888 (1985).
15. D. Done and D. G. Baird, *Polymer,* **30,** 989 (1990).
16. B. Y. Shin, S. H. Jang, I. J. Chung, and B. S. Kim, *Polym. Eng. Sci.,* **32,** 73 (1992).
17. M. M. Miller, J. M. G. Cowie, J. G. Tait, D. L. Brydon, and R. R. Mather, *Polym. Eng. Sci.,* **36,** 3107 (1995).
18. Y. P. Chiou, K. C. Chiou, and F. C. Chang, *Polym. Eng. Sci.,* **37,** 4099 (1996).
19. A. Datta and D. G. Baird, *Polymer,* **36,** 505 (1995).
20. H. J. O'Donnell and D. G. Baird, *Polymer,* **36,** 3113 (1995).
21. S. C. Tjong, S. X. Chen, and R. K. Y. Ki, *J. Appl. Polym. Sci.,* **64,** 707 (1997).
22. G. I. Taylor, *Proc. R. Soc. A,* **146,** 501 (1934).

23. D. E. Turek, G. P. Simon, C. Tiu, O. T. Siang, and E. Kosior, *Polymer,* **33,** 4322 (1992).
24. T. Limtasiri and A. I. Isayev, *J. Appl. Polym. Sci.,* **42,** 2923 (1991).
25. Y. Z. Meng and S. C. Tjong, *Polymer,* to appear.
26. M. J. R. Catelum and N. J. Wagner, *J. Appl. Polym. Sci.,* **34,** 2433 (1996).
27. J. C. Malzahn and K. Friedrich, *J. Mater. Sci. Lett.,* **3,** 861 (1984).
28. M. L. Shiao, S. V. Nair, P. D. Garrett, and R. E. Pollard, *Polymer,* **35,** 306 (1994).
29. T. J. Hutley and M. W. Darlington, *Polym. Commun.,* **25,** 226 (1984).
30. P. M. McGenity, J. J. Hooper, C. D. Paynter, A. M. Riley, C. Nutbeem, N. J. Elton, and J. M. Adams, *Polymer,* **33,** 5215 (1992).
31. T. Ozawa, *Polymer,* **19,** 150 (1971).
32. K. Engberg, M. Ekblad, P. E. Werner, and U. W. Gedde, *Polym. Eng. Sci.,* **34,** 1346 (1994).
33. J. K. Kardos, *J. Adhes.,* **5,** 119 (1973).
34. G. P. Desio and L. Rebenfeld, *J. Appl. Polym. Sci.,* **44,** 1989 (1992).